Submitted: 13.01.2022
Accepted: 24.03.2022
Early publication date: 18.07.2022

Endokrynologia Polska
DOI: 10.5603/EP.a2022.0042
ISSN 0423–104X, e-ISSN 2299–8306
Volume/Tom 73; Number/Numer 4/2022

In-bore MR prostate biopsy — initial experience

Justyna Rembak-Szynkiewicz[1], Piotr Wojcieszek[2], Anna Hebda[1], Patrycja Mazgaj[1], Arkadiusz Badziński[3, 4], Gabriela Stasik-Pres[1], Ewa Chmielik[5], Barbara Bobek-Billewicz[1]

[1]*Radiology and Diagnostic Imaging Department, Maria Skłodowska-Curie National Research Institute of Oncology, Gliwice Branch, Poland*
[2]*Brachytherapy Department, Maria Skłodowska-Curie National Research Institute of Oncology, Gliwice Branch, Poland*
[3]*Department of Histology and Cell Pathology, Medical University of Silesia, Katowice, Poland*
[4]*Institute of Linguistics, University of Silesia, Katowice, Poland*
[5]*Tumor Pathology Department, Maria Skłodowska-Curie National Research Institute of Oncology, Gliwice Branch, Poland*

Abstract

Introduction: The introduction of multiparametric MRI (mpMRI) has been a breakthrough in the diagnosis of noninvasive clinically significant prostate cancer. Currently, MR-guided prostate biopsy (in-bore biopsy) is the only biopsy method that uses real-time MRI in patients with suspected prostate cancer. The aim of the study was a retrospective analysis of the correlation between MRI results and histological findings of prostate samples suspected of malignancy, which were taken during MRI-guided biopsy.

Material and methods: Thirty-nine patients with 57 lesion biopsies were enrolled in the study. Patients were aged 48–84 years (mean age 67.2 ± 9.4 years).

Results: Cancer was histologically confirmed in 24 lesions, including primary cancer in 14 lesions and local recurrence in 10 lesions. Cancer was not detected in the remaining lesions (n = 33). Malignancy was confirmed in 90% of lesions previously reported as PI-RADS 5. Only one Prostate Imaging and Reporting and Data System (PI-RADS 5) lesion was histologically negative (prostatitis). Cancer was detected in 50% of lesions defined as PI-RADS 4. Cancer cells were not found in any of 23 lesions defined as PI-RADS 3 (53.5%). Most of the lesions assessed as PI-RADS 3 were located in the transitional zone (n = 19). Only four PI-RADS 3 lesions were found in the peripheral zone. Large lesions or lesions feasible for cognitive TRUS biopsy were not referred for MRI biopsy, which resulted in a higher proportion of lesions assessed as PI-RADS 3. Fourteen lesions suspected of local recurrence were assessed in our study. Cancer was found in approximately 72% of the lesions.

Conclusions: Performing prostate biopsy under the guidance of real-time MRI allows precise collection of material for histological examination (even from a very small lesion). As a result, both primary cancer and local recurrence after previous radiotherapy of prostate cancer can be confirmed. **(Endokrynol Pol 2022; 73 (4): 712–724)**

Key words: *prostate; imaging-guided biopsy; core-needle biopsy; multiparametric magnetic resonance imaging; magnetic resonance-guided interventional procedures; biopsy; prostate cancer; prostate neoplasms*

Introduction

Prostate cancer is one of the most prevalent malignancies in men [1, 2]. Prostate cancer is mostly hormone-sensitive [3]. Magnetic resonance imagining is the most effective non-invasive method for prostate cancer detection. It should be always performed with the Prostate Imaging and Reporting and Data System (PI-RADS). PI-RADS v. 2.1 has been used since 2019 [4, 5]. Definitive diagnosis of prostate cancer is established based on histological findings from biopsy samples [4].

At present, transrectal ultrasound (TRUS)-guided core biopsy is the most frequently performed procedure [6]. However, the tumour location can be detected only in a small number of cases (≤ 30%) when TRUS is applied [7]. Tissue samples are collected from specific prostate areas with systemic TRUS-guided biopsy. It is often difficult to obtain cancer tissue. This leads to a large percentage of false-negative results, which is related to consecutive biopsies and treatment [6, 8].

The introduction of multiparametric MRI (mpMRI) has been a breakthrough in the diagnosis of noninvasive clinically significant prostate cancer [9–11]. MpMRI with a 3 T scanner enables the most precise prostate assessment. It shows the location of a clinically significant cancer, which allows a targeted biopsy [9].

Biopsies performed with MRI [also known as MR-directed biopsies or magnetic resonance imaging-guided biopsies (MRI-GB)] include cognitive transrectal biopsy (COGTB), MRI-transrectal ultrasound fusion biopsy (FUS-TB), and in-bore MRI transrectal biopsy (MRI-TB) [12]. Of these, COGTB is the most commonly applied after initial MR evaluation [12]. Biopsy is performed under TRUS in correlation with

Dr n. med. Justyna Rembak-Szynkiewicz, Radiology and Diagnostic Imaging Department, Maria Skłodowska-Curie Memorial Cancer Centre and Institute of Oncology, Branch in Gliwice, tel/fax: +48 508135336; e-mail: Justyna.Rembak-Szynkiewicz@io.gliwice.pl, remszyn@wp.pl

MR images, which allows for the identification of suspected lesions. However, it requires considerable experience of the operator both in the assessment of MRI and ultrasound (US). It is insufficient but useful mainly for the detection of large lesions. On the other hand, it is possible to combine COGTB with systematic biopsy [12].

FUS-TB biopsy is a more effective approach. It is used under TRUS guidance after the fusion of US and MRI images. The specialist who performs the biopsy sees both images, which increases the likelihood of collecting cancer samples. The most significant limitation is related to difficulties with the fusion of images obtained from two different modalities [13].

In-bore MRI-TB is considered the most precise in-real time biopsy (preferably using a 3T scanner). A specialized system compatible with the MRI electromagnetic field is required [14]. In-bore biopsy is mostly performed using the transrectal approach with an MRI needle guide connected to a computer-operated robot.

MR sequences allow for the detection of the most suspicious lesions, and the use of the robot allows for the optimal needle position. T2-weighted images and diffusion weighted imaging/apparent diffusion coefficient (DWI/ADC) are performed during MRI-guided biopsy. The prostate cancer is usually characterized by diffusion restriction. The areas suspected of the highest malignancy can be visualized when MRI examination is applied [15].

After correct positioning of the guide, the needle is inserted and the radiologist collects samples from the suspected region(s). Proper positioning of the needle or the biopsy route must be always confirmed and documented on MRI. The procedure, including patient preparation and positioning in the MRI scanner, usually takes approximately 30–60 min, depending on the number of lesions [12, 15]. During an MRI-guided biopsy, usually 2–4 samples are collected from each lesion, which is less than the standard systematic TRUS biopsy. A lower number of obtained samples is associated with a lower risk of biopsy-related complications such as haemorrhage or infection and is connected with better comfort of patients [7].

Currently, in-bore prostate biopsy is one of the methods of MRI-GB in patients suspected of primary prostate cancer. There are several algorithms of procedures and diagnostic strategies in which MRI examination and biopsies are used [7, 9, 14–18].

The aim of the study was a retrospective analysis of the correlation between MRI results and histological findings of prostate samples suspected of malignancy, which were taken during in-bore biopsy.

Material and methods

Thirty-nine patients with 57 lesion biopsies were enrolled in the study. Patients were aged 48-84 years (mean age 67.2 ± 9.4 years). Prostate-specific antigen (PSA) levels in patients with the suspicion of primary cancer ranged from 6.4 to 13.16 ng/mL. PSA levels in patients suspected of local recurrence ranged from 0.86 to 4.45 ng/mL. Single lesions were assessed in 25/39 (64%) patients, 2 lesions in 10/39 (26%) patients, and 3 lesions in 4/39 (10%) patients. The material was collected in the Radiology and Diagnostic Imaging Department, Maria Sklodowska-Curie National Research Institute of Oncology, Gliwice from November 2019 to December 2020.
Patients were divided into 2 subgroups:

— group 1: patients referred for biopsy with the lesions classified as PI-RADS ≥ 3 with the suspicion of primary cancer (43 lesions in 28 patients);
— group 2: patients referred for in-bore biopsy with the suspicion of local recurrence of prostate cancer after radical radiotherapy (14 lesions in 11 patients).

Diagnostic mpMRI prostate examinations performed outside of the Maria Sklodowska-Curie National Research Institute of Oncology were accepted; however, most patients (n = 26) underwent examination using a 3T scanner in the Maria Sklodowska-Curie National Research Institute. The examinations that were performed outside of the Research Centre were sent to the PACS system. Large lesions that were visible on TRUS examination were not referred for MRI biopsy. They were referred to cognitive transrectal ultrasound (TRUS TB – COGTB) after the evaluation made by the radiologists experienced in assessment of MR and TRUS biopsies. Characteristics of the patients and lesions are given in Figures 1 and 2.

Biopsy procedure

In-bore biopsies were performed on a 3T scanner (Magnetom Vida, Siemens Healthineers, Erlangen, Germany). A remote-controlled manipulator RCM (Soteria Medical B, Arnhem, Netherlands) was used for the biopsies.
The remote-controlled manipulator (robot) was positioned between the lower limbs of patients and connected with the controller unit (including a compressor and a computer), which was located in the steering room. The robot and the compressor were connected using plastic tubes. The movement of the robot was controlled by the computer using the pressure difference in the plastic tubes.
The guide, dedicated to the MRI electromagnetic field, was inserted into the rectum and was later connected to the robot.

MRI examination protocol

The protocol includes the following procedures:

— target images to confirm the location of the guide — true fast imaging with steady-state free precession (TRUFI); (sagittal and axial planes aligned with needle MR guide TR 4.6 ms, TR 2.3 ms, sl7, TA 0:12 min and 0:10 min, respectively);
— diagnostic imaging to determine the location of the lesion(s) — t2_tse_tra (TR 4780 ms, TE 112 ms, TA 1:31 min), DWI (b 50, 100, 500, 1000, 1600, 2000 s/mm^2, TR 3100 ms, TE 75 ms, TA 4:02 min);

A dedicated guide and a needle were used for the biopsies:

— plastic guide (MRI Needle Guide 18Gx 150mm, BIP GmbH Am Brand 1, Turkenfeld, Germany);
— and one of the two following needles:
  a) a needle dedicated to the electromagnetic field, needle location can be controlled in the field; semi–automatic biopsy needle (18 G × 200 mm, Innovative Tomography Products GmbH, Bochum, Germany);
  b) an automatic biopsy gun, steel needle, MR automatic biopsy system (Histocore; 18 G × 200 mm BIP GmbH Am Brand 1, Turkenfeld, Germany).

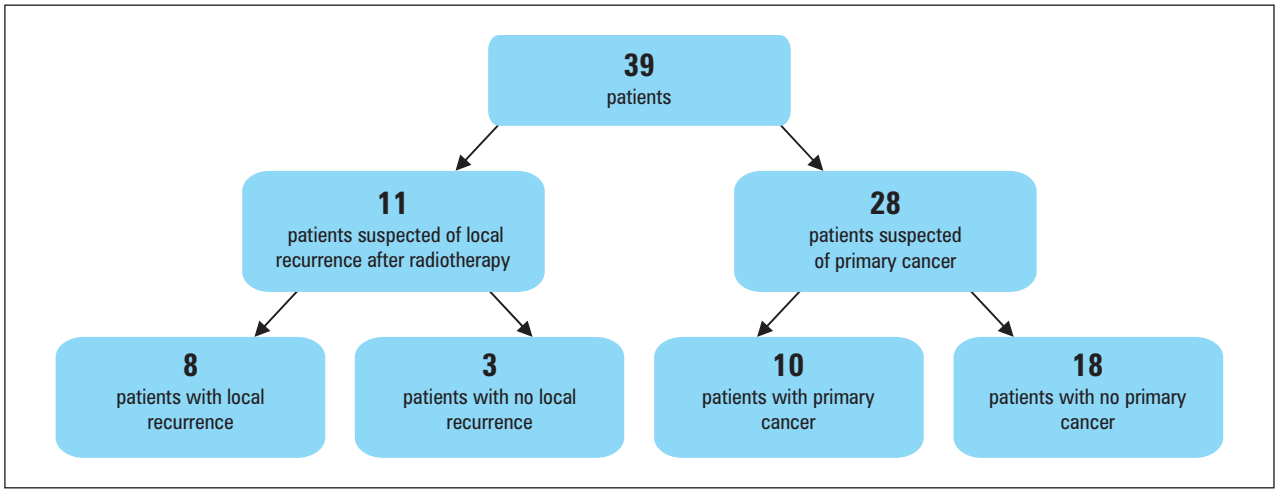

Figure 1. *Patients' characteristics*

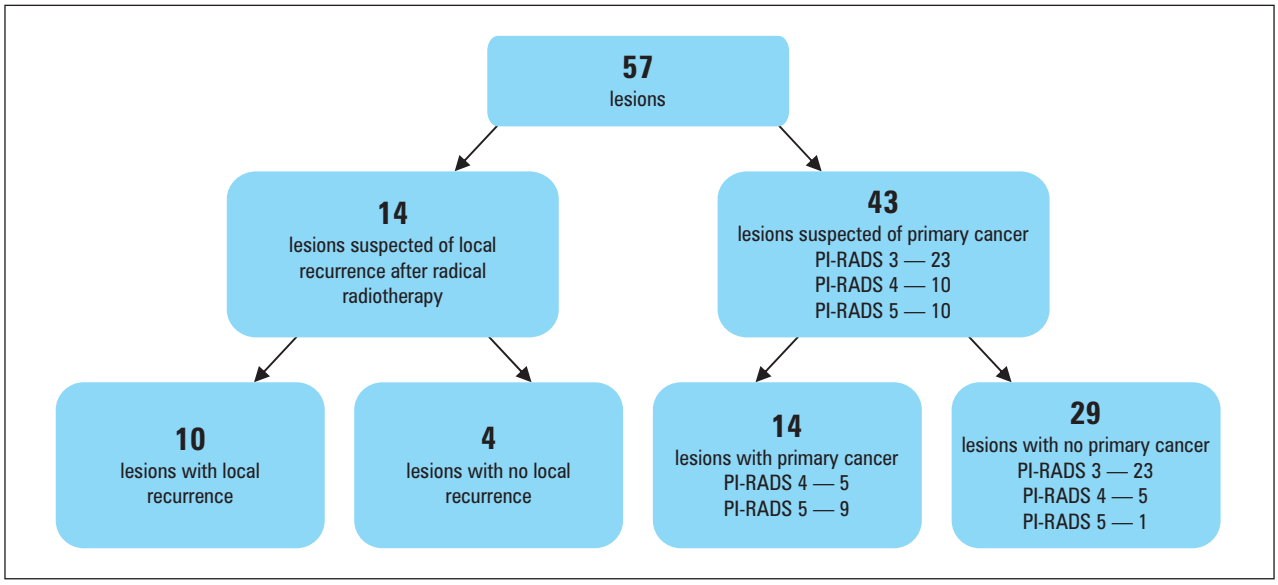

Figure 2. *Lesions characteristics. PI-RADS — Prostate Imaging and Reporting and Data System*

Patient position

Patients were in a prone position. A special pillow was located under the pelvis (2 different sizes of pillows depending on patient anatomy, prostate size, and lesion location). The rectum was anaesthetised topically using a lidocaine gel (Lidocaini hydrochloridum; 20 mg/g; PharmaSwiss, Czech Republic).

Course of the procedure

After the patients were positioned prone and anaesthetised, the guide was inserted into the rectum and connected to the robot. The localizer and very rapid T2-weighted TRUFI sequences were performed (parallel to the guide; sagittal and transverse planes). Next, diagnostic T2-weighted and diffusion-weighted images (DWI) were also done. The position of the guide was calibrated, and the target lesion suspected of cancer was determined. Next, the robot was activated and re-located towards the lesion. The correct positions of the guide and the trajectory were confirmed using TRUFI sequences. Next, the biopsy sample was collected by a radiologist. The same protocol was repeated to obtain biopsy samples from different lesion locations.

Patient preparation

Patients were prepared for the procedure (transrectal enema, implementation of oral antibiotic therapy one day prior to the procedure; blood tests, including complete blood count and blood clotting tests). Whenever possible, patients were asked to discontinue anticoagulants prior to biopsy. Low-molecular-weight heparin was not contraindicated. However, heparin was not administered on the day of the biopsy. The final decision related to the discontinuation or change in therapy was taken by a general practitioner or a cardiologist prior to biopsy.

After the procedure, patients were monitored in the Department of Radiology for 3 hours. Biopsy-related adverse effects included malaise at the time of biopsy (n = 2), which required termination of the procedure (but not hospitalization). Following the consultation, asymptomatic patients were discharged home. No early- or late-onset complications were reported.

Histological assessment

Two to five samples were taken from each lesion. They were embedded in formalin and sent to the Department of Cancer Pathology,

National Research Institute of Oncology, Gliwice, Poland. Tissue samples were fixed for 12-24 hours, and histological evaluation was performed. The samples were embedded in paraffin and cut on the microtome into 3-μm sections. Histological samples were stained with haematoxylin and eosin (H + E).

Statistical analysis

Mean values for variables with normal distribution and median values for variables with non-normal distribution with the data on the prevalence in subgroups are given in Tables 1 and 4. Kruskal-Wallis One-Way ANOVA rank test was used for the differential analysis for independent samples, and the post-hoc test was applied for multiple comparisons. The χ^2 test was used to verify the size of the subgroups, depending on the selected variables. The level of statistical significance was established at $\alpha = 0.05$. Statistica v. 12 was used for the analysis.

Results

Group analysis

Histological evaluation was performed, and cancer was detected in 18/39 (46%) patients, whereas malignancy was not confirmed in 21/39 (54%) patients.

11/39 (28%) patients underwent biopsy due to the suspicion of local recurrence (cancer was confirmed in 8 patients, while malignancy was not histologically detected in 3/11 patients).

Biopsy was collected from 28/39 patients due to the suspicion of primary cancer, which was confirmed in 10/39 (26%) subjects, and 18/39 patients did not present with primary cancer. Benign prostate hyperplasia and prostatitis were histologically confirmed.

Fifty-seven lesions were assessed. Histological findings were as follows: primary cancer was found in 14 lesions, local recurrence in 10 lesions, and cancer was not detected in the remaining lesions (n = 33).

Histological characteristics are given in Figure 3.

Analysis of histological findings

Cancer was histologically confirmed in 24 lesions. Malignancy was confirmed in 90% of lesions previously reported as PI-RADS 5. Cancer cells were not found in any of the 23 lesions defined as PI-RADS 3. Cancer was detected in 50% of the lesions defined as PI-RADS 4.

Cancer was confirmed in 10/14 patients in most lesions suspected of recurrence (71.4%) following radiation therapy. Table 1 shows the number of malignant lesions confirmed by in-bore biopsy.

Analysis of PSA results

PSA levels of patients ranged from 0.86 to 13.16 ng/mL (median 6.83 ng/mL). These levels were significantly lower in the group suspected of recurrence (2.91 ng/mL) compared to the group with confirmed primary tumour (10.30 ng/mL) and the group with no

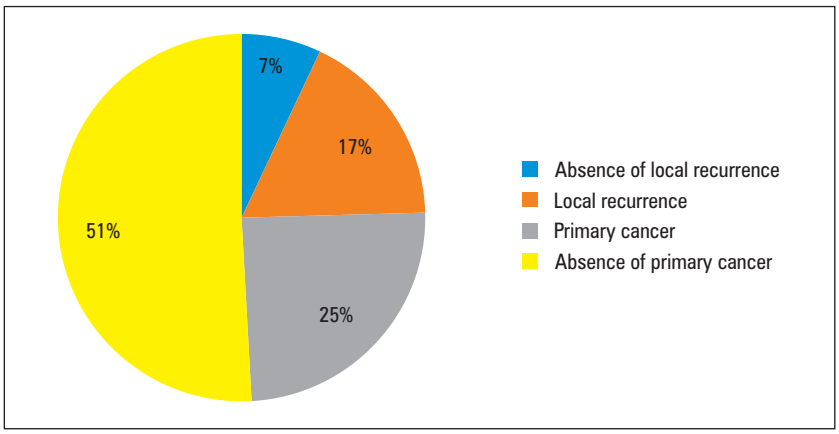

Figure 3. *Histological findings*

Table 1. *Lesions confirmed by in-bore biopsy*

MRI results	Non-malignant lesions (n = 33; 58%)	Malignant lesions (n = 24; 42%)
PI-RADS 3	23	0
PI-RADS 4	5	5
PI-RADS 5	1	9
Suspicion of local recurrence on MRI	4	10

PI-RADS — Prostate Imaging Reporting and Data System; MRI — magnetic resonance imaging

primary cancer (8.99 ng/mL) ($p < 0.001$). No significant PSA differences were found between the group with primary cancer and the group with no cancer (Tab. 2). Detailed patient characteristics are given in Table 2.

Analysis of lesion size

The mean size of lesions was 12.7 mm (SD ± 5.2 mm). The recurrence lesions were significantly smaller (9.8 mm) compared to primary cancer (15.6 mm) ($p = 0.016$). The results are given in Table 3.

Analysis of lesion location

Most primary lesions (23/43) were localized in the transitional zone, and malignant lesions were confirmed only in 7% of the lesions. However, most malignancies were detected in the peripheral zone (Fig. 4–6).

Assessment of MRI findings

T2-weighted images

T2-weighted images for lesions suspected of primary cancer are given in Table 4.

Table 2. *Patients' characteristics*

	Patients with confirmed local recurrence (n = 8)	Patients in whom local recurrence was not confirmed (n = 3)	Patients with confirmed primary cancer (n = 10)	Patients in whom primary cancer was not confirmed (n = 18)
Mean age [years] ± SD	70 ± 10	67 ± 8	68.2 ± 9.2	64.4 ± 9.5
Median PSA [ng/mL]	2.91	2.50	10.30	8.99
Quartile range	2.31–4.17	0.86–4.45	6.40–13.16	6.79–12.00
Time between MRI examination and biopsy [months]	1.40	0.85	2.03	1.4
Interquartile range	1.10–2.23	0.68–1.24	1.16–5.35	0.9–2.4

SD — standard deviation; PSA — prostate-specific antigen; MRI — magnetic resonance imaging

Table 3. *Comparison of variables between the cancer group and the non-cancer group*

	Lesions with no primary cancer (n = 29)	Lesions with primary cancer (n = 14)	Lesions with local recurrence (n = 10)	Lesions with no local recurrence (n = 4)
Mean largest lesion dimension [mm] ± SD	12.5 ± 5.7	15.6 ± 4.6	9.8 ± 3.0	11.3 ± 3.4

SD — standard deviation

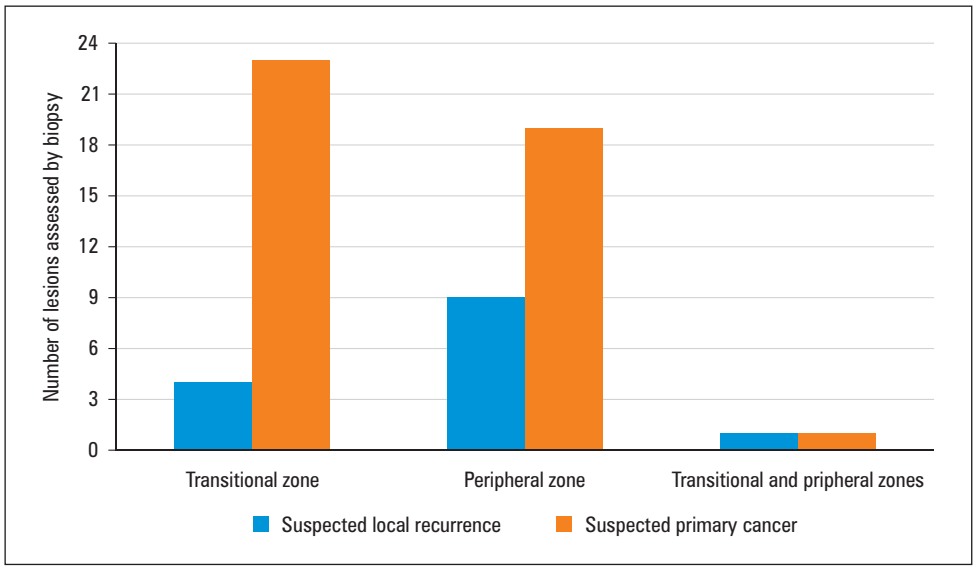

Figure 4. *Number of lesions depending on their location*

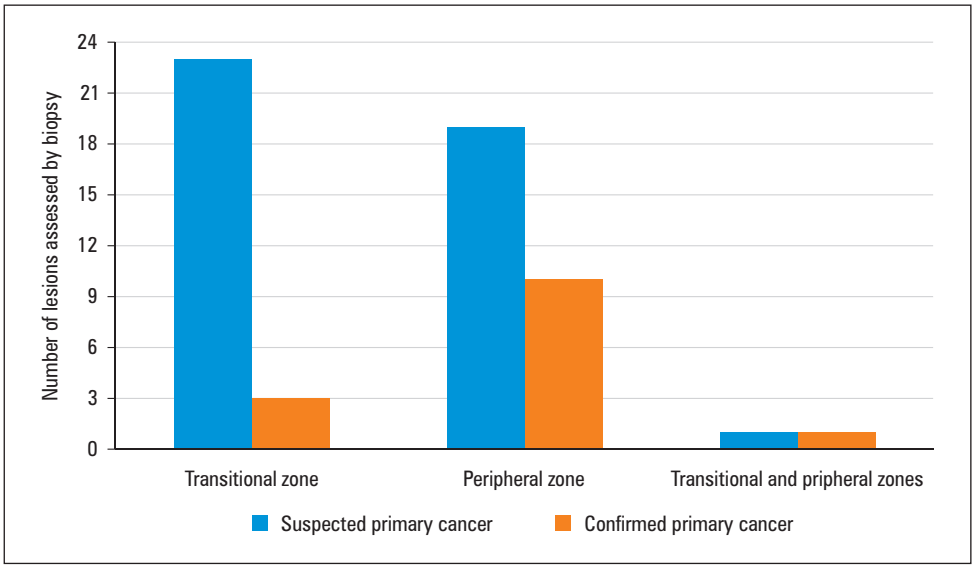

Figure 5. *All lesions suspected of primary cancer with their location*

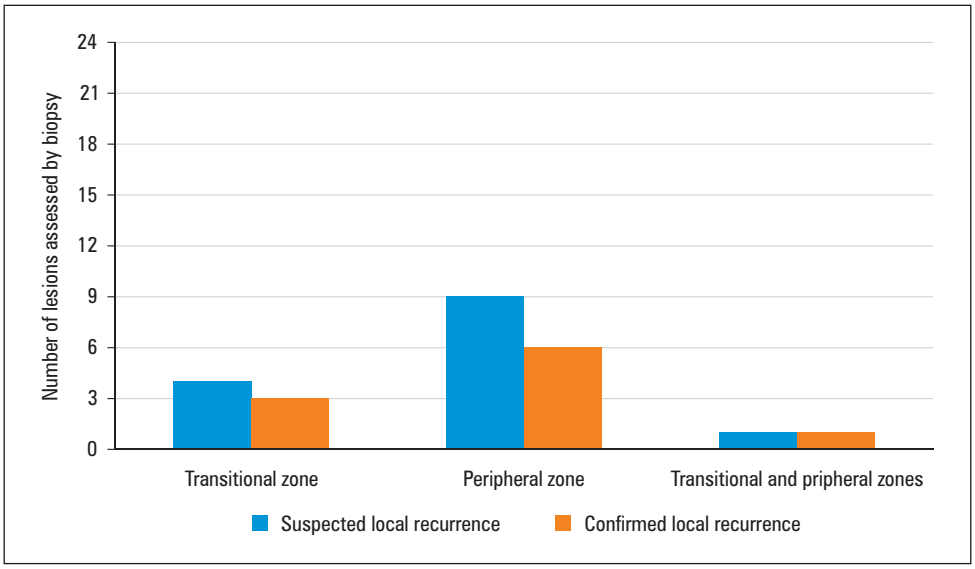

Figure 6. *All lesions suspected of local recurrence with their location*

Table 4. ***Prostate Imaging Reporting and Data System (PI-RADS) score on T2-weighted images.***

T2-weighted images score	Lesions with no primary cancer (n = 29)	Primary cancer (n = 14)
2	3	0
3	19	0
4	5	4
5	2	10

PI-RADS = 3 on T2-weighted images was predominant (65%) in the group in whom cancer was not detected whereas PI-RADS = 5 was found for malignant lesions in 72% ($p < 0.001$).

DWI images

Primary cancer scored as PI-RADS 4 or PI-RADS 5 on DWI was found in 13/14 lesions. Only one primary cancer had PI-RADS 3. PI-RADS 3 was mostly found in non-malignant lesions (55%; Tab. 5).

Diffusion restriction is characteristic of malignancy, i.e. high signal intensity (SI) on DWI $b_{max} \geq 1400$ s/mm^2 and low SI on the ADC map. All malignant lesions were characterized by diffusion restriction. No diffusion restriction was found in 16/29 (55%) benign lesions,

Table 5. *Prostate Imaging Reporting and Data System (PI-RADS) score on diffusion-weighted imaging (DWI)*

DWI score	Non-malignant lesions (n = 29)	Malignant lesions (n = 14)
2	6	0
3	16	1
4	6	5
5	1	8

Table 6. *Restriction diffusion on diffusion-weighted imaging (DWI)*

DWI/ADC	Non-malignant lesions (n = 29)	Malignant lesions (n = 14)
Non-restricted diffusion	16	0
Diffusion restriction	13	14

ADC — apparent diffusion coefficient

whereas diffusion restriction was reported in 13/29 (45%) non-malignant lesions (Tab. 6).

Discussion

In-bore prostate biopsy a method of magnetic resonance imaging-guided biopsies (MRI-GB) that allows precise collection of tissue samples suspected of cancer for histological assessment [9, 14, 15]. However, many studies showed a large discrepancy in detecting primary cancer using in-bore biopsy. Detection rates range from 37% to 73% for PI-RADS ≥ 3. These results were significantly better for PI-RADS 4 and 5, and reached as much as 88% [15, 19]. In our study, the rate was 46% for PI-RADS ≥3 and 70% for PI-RADS 4 and 5 (Fig. 7AB).

Twenty-three lesions assessed as PI-RADS 3 were suspected of primary cancer (53.5%). Most of them were located in the transitional zone (n = 19).

Only 4 PI-RADS 3 lesions were found in the peripheral zone. According to the American Congress of Radiology, PI-RADS 3 is inconclusive and hence difficult for clear assessment, especially if localized in the transitional zone [4, 5].

Nodules in the transitional zone are often characterized by diffusion restriction. However, it does not have to be related to malignancy. In some benign nodules, diffusion restriction can mimic cancer, considering the structure and an increase in the number of cells in the nodule [20–22]. Therefore, PI-RADS 2.1 is the revised version used for the assessment of lesions in the transitional zone. How-

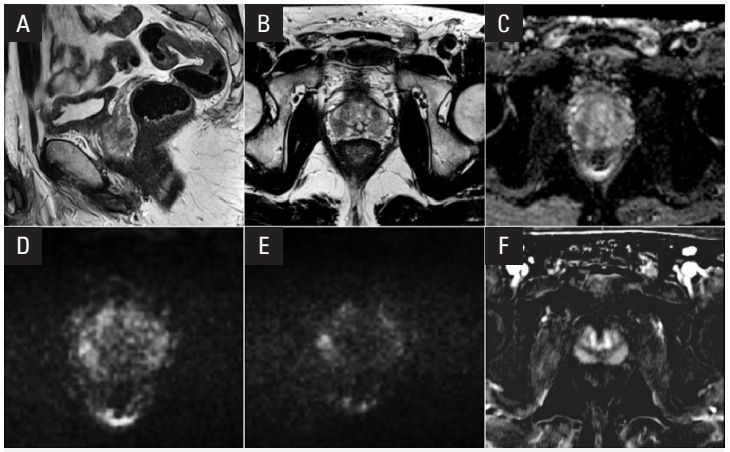

T2-weighted images, sagittal plane, hypointense lesion (A), T2-weighted images, axial plane, hypointense lesion (11 mm), right peripheral zone (B), ADC map, diffusion restriction, ADC 0.46 × 10^{-3}mm²/s (C), DWI b 1000 s/mm², axial plane, hyperintense lesion (D), DWI b 2000 s/mm² axial plane, hyperintense lesion (E), DCE lesion is poorly visible against the background of highly enhanced peripheral zone (F)

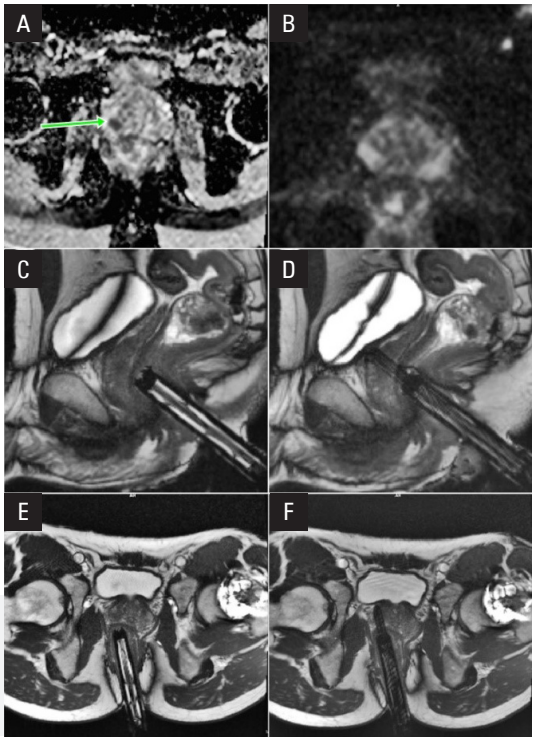

ADC map, diffusion restriction (arrow) (A), DWI b 1000 s/mm², hyperintense lesion (B), T2-weighted images, sagittal plane, prior to the needle insertion (C), T2-weighted images, sagittal plane, with the needle insertion (D), T2-weighted images, oblique axial plane, prior to the needle insertion (E), T2-weighted images, oblique axial plane, correct position of the needle in the prostate (F)

Figure 7. *Patient aged 64 years with suspicion of primary cancer. Prostate-specific antigen (PSA) 6.4 ng/mL, free PSA (fPSA) 0.582 ng/mL, digital rectal exam (DRE) — negative. Transrectal ultrasound (TRUS) biopsy — negative.* **A.** *Diagnostic magnetic resonance imaging (MRI), lesion PI-RADS 4;* **B.** *In-bore biopsy, histopathology (HP) — adenocarcinoma Gleason score 6 (3+3); prognostic group: 1, cancer tissue samples 60%. ADC — apparent diffusion coefficient; DWI — diffusion-weighted imaging; DCE — dynamic contrast enhancement*

ever, there are still problems related to the interpretation of the lesions in the transitional zone [4].

In our study, histological evaluation of all PI-RADS 3 lesions showed no malignancy. Vilanova et al. found 20% of cancers for PI-RADS 3 lesions using robot-assisted transrectal MRI-guided biopsy [15]. In other studies, including PRECISION, the detection rates ranged from 6 to 20% and were related to the quality of MRI, the experience of the investigator, the biopsy type, and the disease prevalence in the population. Therefore, detection rates were higher and reached as much as 33% in non-naïve men [23, 24].

In our group, large lesions or lesions feasible for cognitive TRUS biopsy were not referred for MRI biopsy, which resulted in a higher proportion of lesions assessed as PI-RADS 3.

Studies have shown that cognitive biopsy can be useful, mainly when lesions are localized in the posterior peripheral zone (for lesions assessed as PI-RADS 4 and 5, 80–88% of them were visible on second-look TRUS) [25, 26].

Histological reports should be correlated with MRI PI-RADS score. However, MRI evaluation must be performed again if histological assessment does not correspond to PI-RADS. In specific cases, second MRI with second biopsy should be performed if clinically indicated.

In our study, only one PI-RADS 5 lesion was histologically negative (prostatitis). The lesion resolved and was not found on follow-up MRI 3 months later. Additionally, PSA level was not elevated in 4 negative PI-RADS 4 lesions in the follow-up, the progression of lesions was not reported, and some lesions were even more difficult to detect on follow-up MRI.

One of the largest studies on in-bore biopsy was conducted by Pokorny et al. [27], in which 607 targets in 554 men were biopsied. The findings showed that the overall cancer detection rate was 80% in patients and 76% in lesions. PI-RADS 3, 4, and 5 demonstrated cancer in 36%, 79%, and 97%, respectively.

Pokorny et al. [27] also reviewed the literature on in-bore biopsy from 2013 to 2018. Twenty-three studies were analysed, in which 4061 patients underwent MRGB. Cancer was detected in from 38 to 80% of patients. Only 9 studies assessed cancer detection depending on the PI-RADS results — PI-RADS 3 (6–49%), PI-RADS 4 (34–77%), and PI-RADS 5 (82–96.3%).

Vural et al. [28] assessed PI-RADS 4 and 5 in 246 patients who had undergone in-bore biopsy. The overall prostate cancer detection rates were 80.5% per patient and 78% per target. The detection rate was 68% and 92% in PI-RADS 4 and 5, respectively.

Additionally, those authors compared the literature on in-bore biopsy from 2018 to 2021 in 10 papers, in which the overall detection cancer ranged from 45.6 to 84%, for PI-RADS 4 from 48.6% to 78%, while 87.5 to 97% for PI-RADS 5.

D'Agostino et al. [29] showed a comparable value of in-bore bore and FUS-TB biopsy. After analysing the target biopsy in 297 patients, those authors did not observe the clear superiority of one technique over another. The lesion site and localization were equally comparable among 2 groups. The overall detection rate was similar (45.5% of the FUS-TB group *vs*. 52.8% of the "in-bore" group). Histological ISUP grade was also comparable among 2 groups. Furthermore, it should be noted that in-bore biopsy is characterized by real-time feedback in needle placement, fewer sampled cores, and a low likelihood of missed target. Additionally, it has the potential to reduce the sampling error related to unselective standard biopsy scheme by providing better disease localization.

In 2017, in their meta-analysis, Wegelin et al. [30] analysed 43 studies and found that MRI-GB allowed the detection of more clinically significant cancers compared to TRUS biopsy. Statistically significant higher sensitivity was detected when in-bore biopsy was used as compared to COGTB. However, no statistically significant difference was found between FUS-TB and COGTB or between FUS-TB and MRI-TB.

In the case of clinically significant cancer, sensitivity of in-bore biopsy was 0.92, 0.89 in the case of FUS-TB, and 0.86 for COGTB. A large limitation of this meta-analysis was the lack of PI-RADS assessment. Additionally, the size and location of lesion were not assessed, which is of crucial importance when biopsy methods are compared.

Prince et al. [31] assessed 286 men (191 in-bore biopsy, 95 FUS-TB). In-bore MRI-targeted prostate biopsy was connected with significantly greater likelihood of target-specific detection of prostate cancer and with non-significantly higher likelihood of target-specific detection of ISUP GG2 or more advanced prostate cancer than is FUS-TB.

There are still too few reports related to the verification of prostate lesions that are suspected of local recurrence after radiation therapy.

Currently, biochemical recurrence is reported in as much as 50% of patients within 10 years after undergoing external-beam radiotherapy (EBRT) for prostate cancer [32].

Microscopic confirmation of local recurrence may provide crucial information before salvage treatment [33]. Such therapy may be beneficial for relapsing patients, but it is related to a higher probability of adverse events. Therefore, patients should be selected for salvage brachytherapy, salvage prostatectomy, and other invasive procedures very carefully [32–37].

Prostate assessment using TRUS following radiation therapy is very difficult. From our experience, the post-radiation prostate is very often a small, non-homogeneous hypoechogenic structure. From the practical point of view, it is not possible to indicate active cancer. The recurrence is best seen on MRI, particularly on diffusion imaging as the diffusion restriction. Next to T2-weighted images, DWI/ADC sequences are also performed during biopsy. Therefore, it is possible to precisely localize the suspected area and collect samples (Fig. 8AB, 9AB).

Fourteen lesions suspected of local recurrence were assessed in our study. Cancer was found in approximately 72% of the lesions (Fig. 10AB). The smallest lesion was of 5 mm. PET PSMA was performed in negative biopsy patients suspected of local relapse in whom malignancy was not confirmed histologically. PET PSMA results were negative. Additionally, PSA level was not elevated in patients during the follow-up. Patients were under oncological surveillance.

Conclusions

Multiparametric MRI shapes modern oncology. There is a need for good quality images assessed by experienced specialists. Moreover, a wide range of different biopsy techniques may allow for the most reliable histological results. It is our first study to demonstrate the experience related to in-bore prostate biopsy whose results are promising. Further studies are warranted to confirm the usefulness of this method.

Conflicts of interest

The authors declare no conflict of interest.

Funding

This research received no external funding.

References

1. Culp MB, Soerjomataram I, Efstathiou JA, et al. Recent Global Patterns in Prostate Cancer Incidence and Mortality Rates. Eur Urol. 2020; 77(1): 38–52, doi: 10.1016/j.eururo.2019.08.005, indexed in Pubmed: 31493960.
2. Logothetis CJ, Aparicio A, Koinis F, et al. Prostate Cancer: Quo Vadis? Eur Urol. 2019; 76(6): 709–711, doi: 10.1016/j.eururo.2019.06.031, indexed in Pubmed: 31300238.
3. Komura K, Sweeney CJ, Inamoto T, et al. Current treatment strategies for advanced prostate cancer. Int J Urol. 2018; 25(3): 220–231, doi: 10.1111/iju.13512, indexed in Pubmed: 29266472.
4. Rosenkrantz AB, Turkbey B, Barentsz J, et al. Prostate Imaging Reporting and Data System Version 2.1: 2019 Update of Prostate Imaging Reporting and Data System Version 2. Eur Urol. 2019; 76(3): 340–351, doi: 10.1016/j.eururo.2019.02.033, indexed in Pubmed: 30898406.
5. PI-RADS ™ Prostate Imaging — Reporting and Data System 2015 version 2. American College of Radiology.
6. Cheng X, Xu J, Chen Y, et al. Is Additional Systematic Biopsy Necessary in All Initial Prostate Biopsy Patients With Abnormal MRI? Front Oncol. 2021; 11: 643051, doi: 10.3389/fonc.2021.643051, indexed in Pubmed: 33718240.
7. Schoots IG, Padhani AR, Rouvière O, et al. Analysis of Magnetic Resonance Imaging-directed Biopsy Strategies for Changing the Paradigm of Prostate Cancer Diagnosis. Eur Urol Oncol. 2020; 3(1): 32–41, doi: 10.1016/j.euo.2019.10.001, indexed in Pubmed: 31706946.
8. Exterkate L, Wegelin O, Barentsz JO, et al. Is There Still a Need for Repeated Systematic Biopsies in Patients with Previous Negative Biopsies in the Era of Magnetic Resonance Imaging-targeted Biopsies of the Prostate? Eur Urol Oncol. 2020; 3(2): 216–223, doi: 10.1016/j.euo.2019.06.005, indexed in Pubmed: 31239236.
9. Wegelin O, van Melick HHE, Hooft L, et al. Comparing Three Different Techniques for Magnetic Resonance Imaging-targeted Prostate Biopsies: A Systematic Review of In-bore versus Magnetic Resonance Imaging-transrectal Ultrasound fusion versus Cognitive Registration. Is There a Preferred Technique? Eur Urol. 2017; 71(4): 517–531, doi: 10.1016/j.eururo.2016.07.041, indexed in Pubmed: 27568655.
10. Venderink W, van der Leest M, van Luijtelaar A, et al. Results of Targeted Biopsy in Men with Magnetic Resonance Imaging Lesions Classified Equivocal, Likely or Highly Likely to Be Clinically Significant Prostate Cancer. Eur Urol. 2018; 73(3): 353–360, doi: 10.1016/j.eururo.2017.02.021, indexed in Pubmed: 28258784.
11. Schoots IG, Padhani AR. Delivering Clinical impacts of the MRI diagnostic pathway in prostate cancer diagnosis. Abdom Radiol (NY). 2020; 45(12): 4012–4022, doi: 10.1007/s00261-020-02547-x, indexed in Pubmed: 32356003.
12. Venderink W, Bomers JG, Overduin CG, et al. Multiparametric Magnetic Resonance Imaging for the Detection of Clinically Significant Prostate Cancer: What Urologists Need to Know. Part 3: Targeted Biopsy. Eur Urol. 2020; 77(4): 481–490, doi: 10.1016/j.eururo.2019.10.009, indexed in Pubmed: 31791623.
13. Perlis N, Lawendy B, Barkin J. How I Do It — MRI — ultrasound fusion prostate biopsy using the Fusion MR and Fusion Bx systems. Can J Urol. 2020; 27(2): 10185–10191, indexed in Pubmed: 32333739.
14. Linder N, Schaudinn A, Petersen TO, et al. In-bore biopsies of the prostate assisted by a remote-controlled manipulator at 1.5 T. MAGMA. 2019; 32(5): 599–605, doi: 10.1007/s10334-019-00751-5, indexed in Pubmed: 31073867.
15. Vilanova JC, Pérez de Tudela A, Puig J, et al. Robotic-assisted transrectal MRI-guided biopsy. Technical feasibility and role in the current diagnosis of prostate cancer: an initial single-center experience. Abdom Radiol (NY). 2020; 45(12): 4150–4159, doi: 10.1007/s00261-020-02665-6, indexed in Pubmed: 32705314.
16. Padhani AR, Barentsz J, Villeirs G, et al. PI-RADS Steering Committee: The PI-RADS Multiparametric MRI and MRI-directed Biopsy Pathway. Radiology. 2019; 292(2): 464–474, doi: 10.1148/radiol.2019182946, indexed in Pubmed: 31184561.
17. Drost FJH, Osses DF, Nieboer D, et al. Prostate MRI, with or without MRI-targeted biopsy, and systematic biopsy for detecting prostate cancer. Cochrane Database Syst Rev. 2019; 4: CD012663, doi: 10.1002/14651858.CD012663.pub2, indexed in Pubmed: 31022301.
18. Barral M, Lefevre A, Camparo P, et al. In-Bore Transrectal MRI-Guided Biopsy With Robotic Assistance in the Diagnosis of Prostate Cancer: An Analysis of 57 Patients. AJR Am J Roentgenol. 2019; 213(4): W171–W179, doi: 10.2214/AJR.19.21145, indexed in Pubmed: 31268734.
19. Ahmed H, Bosaily AES, Brown L, et al. Diagnostic accuracy of multi-parametric MRI and TRUS biopsy in prostate cancer (PROMIS): a paired validating confirmatory study. Lancet. 2017; 389(10071): 815–822, doi: 10.1016/s0140-6736(16)32401-1, indexed in Pubmed: 28110982.
20. Garcia JJ, Al-Ahmadie HA, Gopalan A, et al. Do prostatic transition zone tumors have a distinct morphology? Am J Surg Pathol. 2008; 32(11): 1709–1714, doi: 10.1097/PAS.0b013e318172ee97, indexed in Pubmed: 18769336.
21. Helfrich O, Puech P, Betrouni N, et al. Quantified analysis of histological components and architectural patterns of gleason grades in apparent diffusion coefficient restricted areas upon diffusion weighted MRI for peripheral or transition zone cancer locations. J Magn Reson Imaging. 2017; 46(6): 1786–1796, doi: 10.1002/jmri.25716, indexed in Pubmed: 28383776.
22. Chatterjee A, Watson G, Myint E, et al. Changes in Epithelium, Stroma, and Lumen Space Correlate More Strongly with Gleason Pattern and Are Stronger Predictors of Prostate ADC Changes than Cellularity Metrics. Radiology. 2015; 277(3): 751–762, doi: 10.1148/radiol.2015142414, indexed in Pubmed: 26110669.
23. Mehralivand S, Bednarova S, Shih JH, et al. Prospective Evaluation of PI-RADS™ Version 2 Using the International Society of Urological Pathology Prostate Cancer Grade Group System. J Urol. 2017; 198(3): 583–590, doi: 10.1016/j.juro.2017.03.131, indexed in Pubmed: 28373133.
24. Kasivisvanathan V, Rannikko AS, Borghi M, et al. PRECISION Study Group Collaborators. MRI-Targeted or Standard Biopsy for Prostate-Cancer Diagnosis. N Engl J Med. 2018; 378(19): 1767–1777, doi: 10.1056/NEJMoa1801993, indexed in Pubmed: 29552975.
25. Ukimura O, Marien A, Palmer S, et al. Trans-rectal ultrasound visibility of prostate lesions identified by magnetic resonance imaging increases accuracy of image-fusion targeted biopsies. World J Urol. 2015; 33(11): 1669–1676, doi: 10.1007/s00345-015-1501-z, indexed in Pubmed: 25656687.
26. van de Ven WJM, Sedelaar JP, van der Leest MMG, et al. Visibility of prostate cancer on transrectal ultrasound during fusion with multiparametric magnetic resonance imaging for biopsy. Clin Imaging.

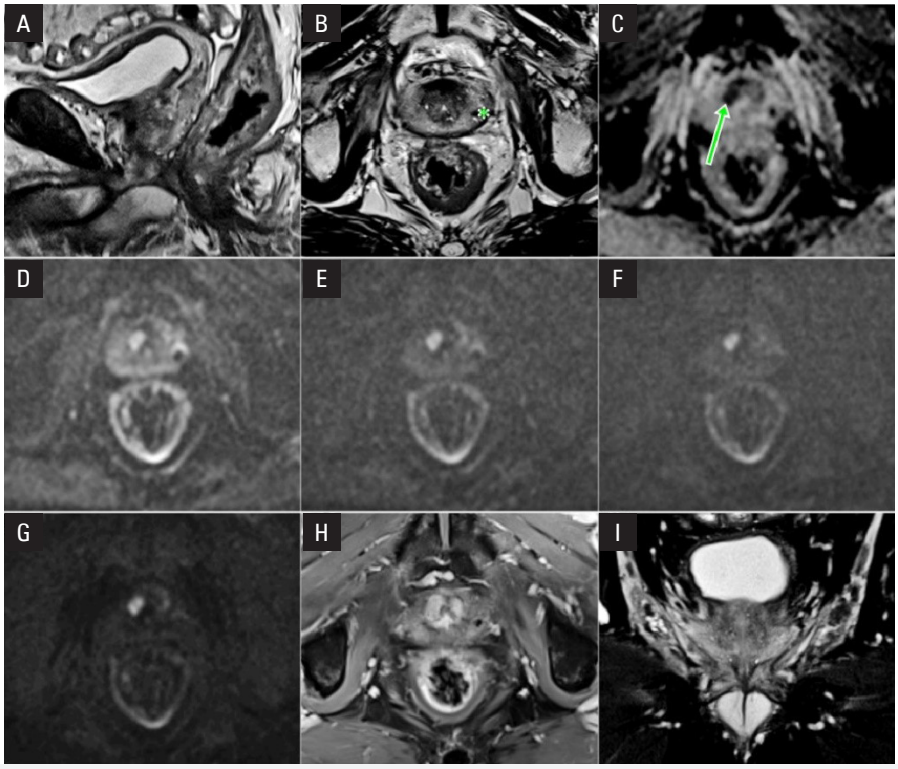

T2-weighted images, sagittal plane, invisible lesion (A), T2-weighted images, axial plane, invisible lesion, (marker for radiotherapy, left peripheral zone) (B), ADC map, diffusion restriction 9mm, ADC 0.46 × 10^{-3} mm^2/s right transitional zone (arrow) (C), DWI b 1000 s/mm^2, axial plane, hyperintense lesion (D), DWI b 1600 s/mm^2, axial plane, hyperintense lesion (E), DWI b 2000 s/mm^2, axial plane, hyperintense lesion (F), calculated b 2500 s/mm^2 (G), DCE, poorly visible lesion against the background of highly enhanced transitional zone (H), T2-weighted, fat-saturated images, coronal plane, invisible lesion (I)

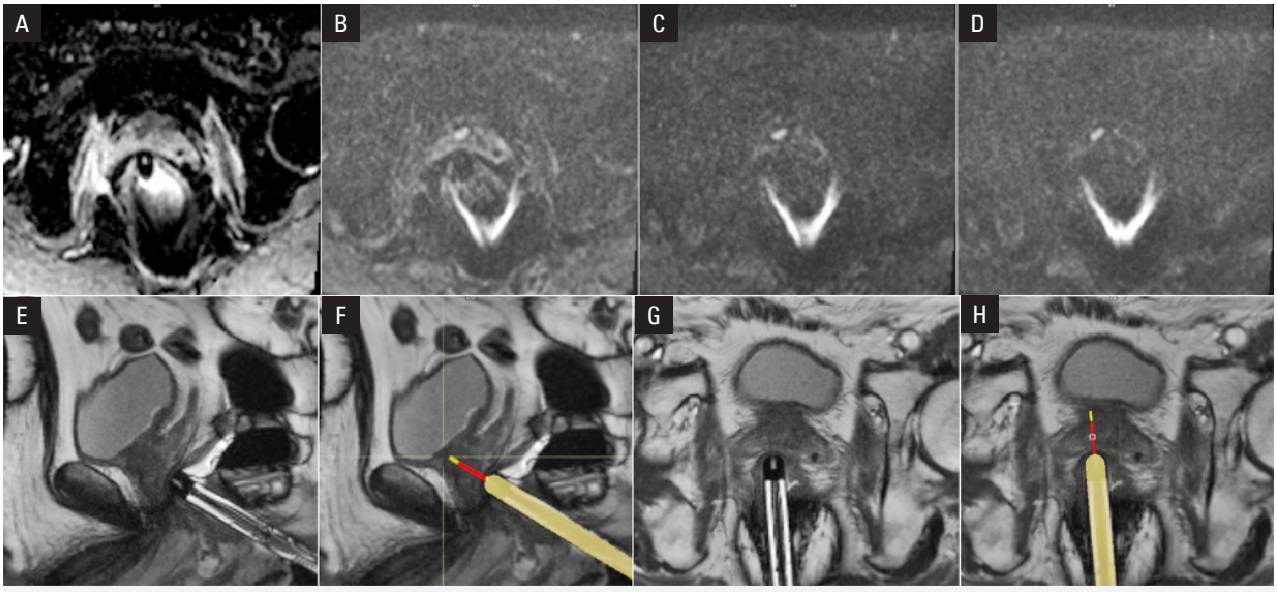

ADC map, diffusion restriction (arrow) (A), DWI b 1000 s/mm^2, axial plane, hyperintense lesion (B), DWI b 1600 s/mm^2, axial plane, hyperintense lesion (C), DWI b 2000 s/mm^2, axial plane, hyperintense lesion (D), T2-weighted images, sagittal plane, prior to the needle insertion (E), T2-weighted images, sagittal plane, biopsy route (the needle track and sample core by yellow and red line) (F), T2-weighted images, axial oblique plane, prior to the needle insertion (G), T2-weighted images, axial oblique plane, biopsy route (the needle track and sample core by yellow and red line) (H)

Figure 8. *Patient aged 82, adenocarcinoma, Gleason score before treatment 6 (3 + 3), prostate-specific antigen (PSA) 22.9 ng/mL diagnosed due to biochemical recurrence, external-beam radiotherapy (EBRT) 7 years prior to recurrence, PSA level at recurrence 3.88 ng/mL.* **A.** *diagnostic magnetic resonance imaging (MRI);* **B.** *In-bore biopsy; histopathology (HP): adenocarcinoma; Gleason score 8 (4 + 4), cancer tissue sample about 40%. ADC — apparent diffusion coefficient; DWI — diffusion-weighted imaging; DCE — dynamic contrast enhancement*

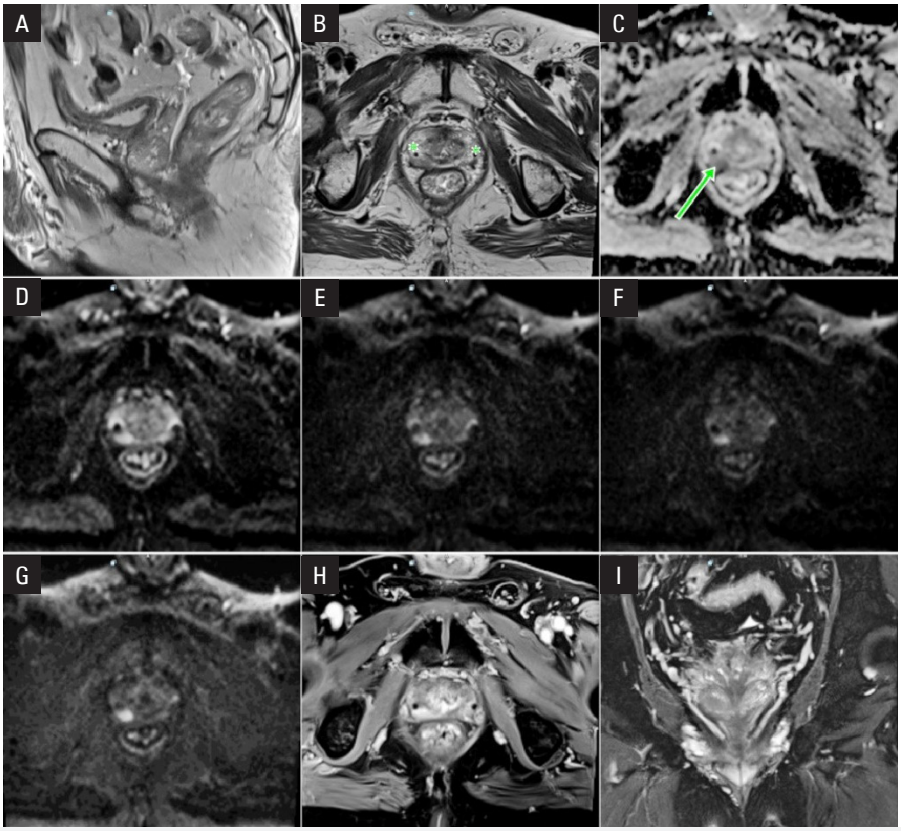

T2-weighted images, sagittal plane (A), T2-weighted images, axial plane, hypointense lesion in the right peripheral zone, (*markers for radiotherapy) (B), ADC map, diffusion restriction 11 mm, ADC 0.46 × 10^{-3} mm^2/s; right peripheral zone (arrow) (C), DWI b 1000 s/mm^2, axial plane, hyperintense lesion (D), DWI b 1600 s/mm^2, axial plane, hyperintense lesion (E), DWI b 2000 s/mm^2, axial plane, hyperintense lesion (F), calculated b 2500 s/mm^2 (G), DCE — lesion enhancement (H), T2-weighted fat-saturated images, coronal plane, hypointense lesion (I)

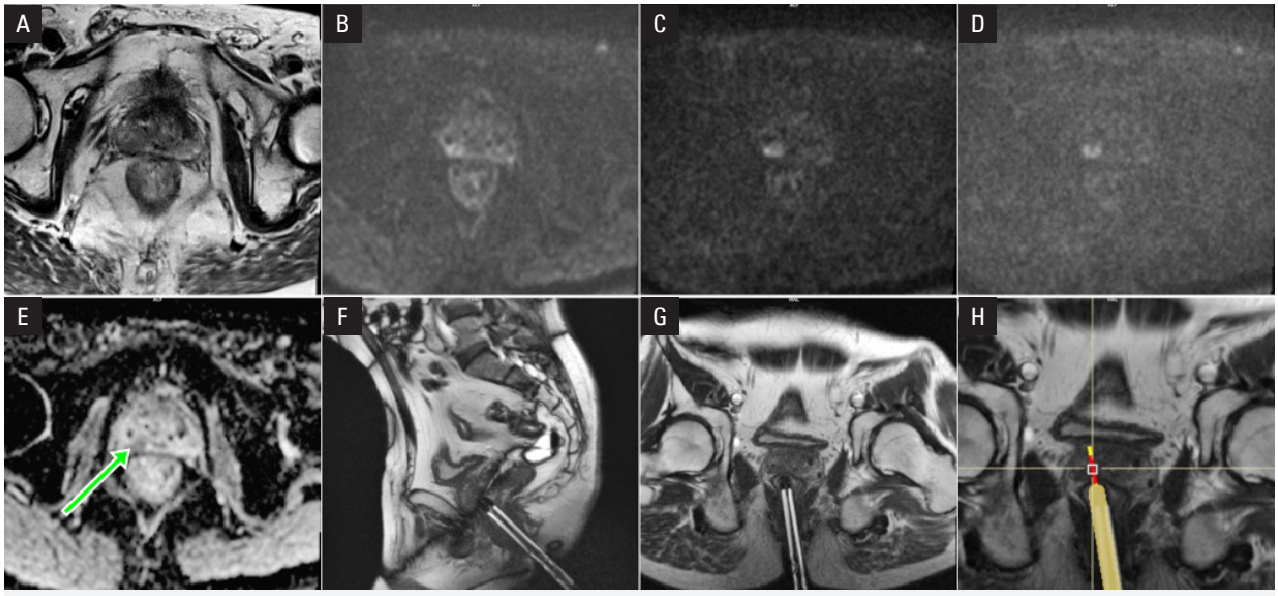

T2-weighted images, axial plane (A), DWI b 1000 s/mm^2, axial plane, hyperintense lesion (B), DWI b 1600 s/mm^2, axial plane, hyperintense lesion (C), DWI b 2000 s/mm^2, axial plane, hyperintense lesion (D), ADC map, diffusion restriction (arrow) (E), T2-weighted images, sagittal plane, prior to the needle insertion (F), T2-weighted images, axial oblique plane, prior to the needle insertion (G), T2-weighted images, axial oblique plane, biopsy route (the needle track and sample core by yellow and red line (H)

Figure 9. *Patient aged 65 years, initial prostate-specific antigen (PSA) prior to treatment 5.42 ng/mL, histopathology (HP): adenocarcinoma, Gleason score 7 (3 + 4), cancer tissue sample 60%, external-beam radiotherapy (EBRT) 5 years before the diagnosis of recurrence (PSA 1.924 ng/mL).* **A.** *Diagnostic magnetic resonance imaging (MRI);* **B.** *In-bore biopsy, HP: adenocarcinoma; Gleason score 8 (4 + 4); grade group 4. ADC — apparent diffusion coefficient; DWI — diffusion-weighted imaging; DCE — dynamic contrast enhancement*

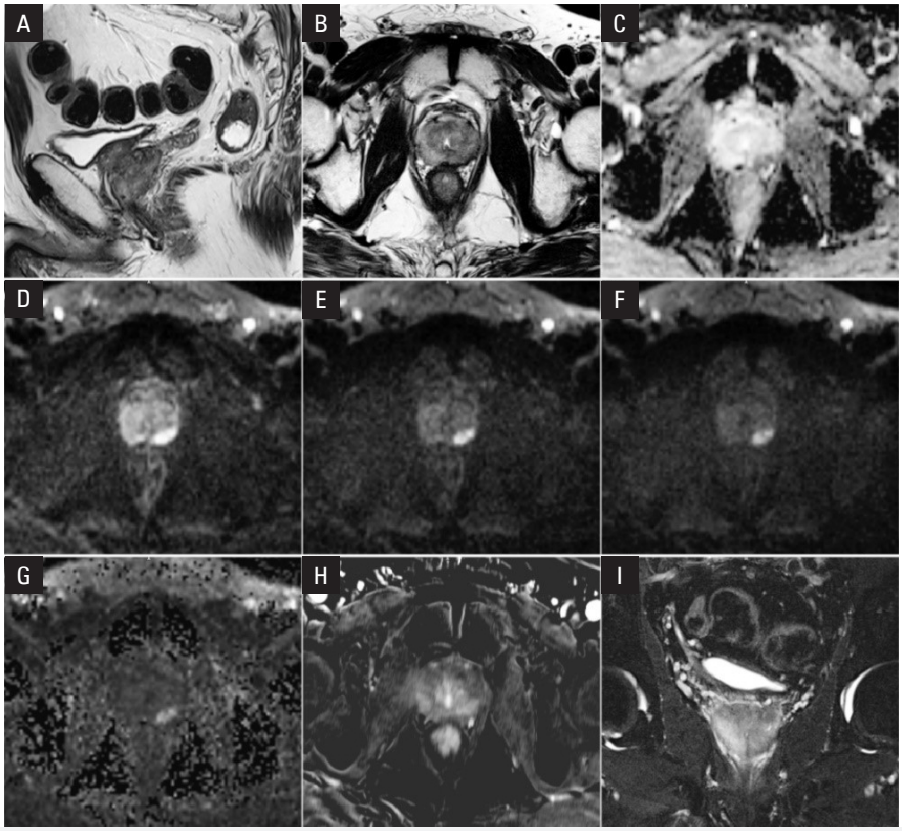

T2-weighted images, sagittal plane (A), T2-weighted images, axial plane, poorly visible lesion (B), ADC map, diffusion restriction 15 mm, ADC 0.6 × 10^{-3} mm^2/s, lesion in left peripheral zone (C), DWI b 1000 s/mm^2, axial plane, hyperintense lesion (D), DWI b 1600 s/mm^2, axial plane, hyperintense lesion (E), DWI b 2000 s/mm^2, axial plane, hyperintense lesion (F), calculated b 2500 s/mm^2 (G), DCE, poorly visible lesion enhancement (H), T2-weighted, fat-saturated images, coronal plane, poorly visible lesion (I)

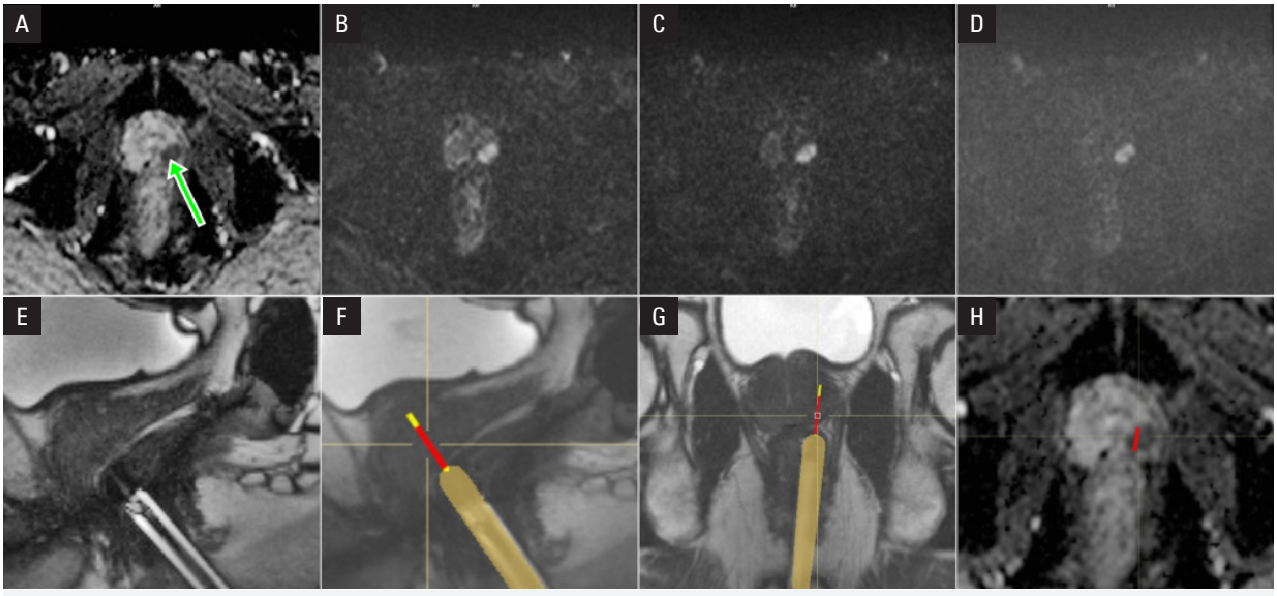

ADC map, diffusion restriction (arrow) (A), DWI b 1000 s/mm^2, axial plane, hyperintense lesion (B), DWI b 1600 s/mm^2, axial plane, hyperintense lesion (C), DWI b 2000 s/mm^2, axial plane, hyperintense lesion (D), T2-weighted images, sagittal plane, prior to the needle insertion (E), T2-weighted images, sagittal plane, biopsy route (the needle track and sample core by yellow and red line) (F), T2-weighted images, axial oblique plane, biopsy route (the needle track and sample core by yellow and red line) (G), ADC map, axial plane, biopsy route (sample core by red line) (H)

Figure 10. *Patient aged 62 years, initial adenocarcinoma Gleason score 7 (3 + 4), brachytherapy; diagnosis 3 years later due to biochemical recurrence, prostate-specific antigen (PSA) at recurrence 3.5 ng/mL.* **A.** *Diagnostic magnetic resonance imaging (MRI);* **B.** *In-bore biopsy, histopathology (HP): adenocarcinoma; Gleason score 7 (4 + 3), prognostic group 3, cancer tissue samples 50%. ADC — apparent diffusion coefficient; DWI — diffusion-weighted imaging; DCE — dynamic contrast enhancement*

2016; 40(4): 745–750, doi: 10.1016/j.clinimag.2016.02.005, indexed in Pubmed: 27317220.
27. Pokorny M, Kua B, Esler R, et al. MRI-guided in-bore biopsy for prostate cancer: what does the evidence say? A case series of 554 patients and a review of the current literature. World J Urol. 2019; 37(7): 1263–1279, doi: 10.1007/s00345-018-2497-y, indexed in Pubmed: 30255394.
28. Vural M, Coskun B, Kilic M, et al. In-bore MRI-guided prostate biopsy in a patient group with PI-RADS 4 and 5 targets: A single center experience. Eur J Radiol. 2021; 141: 109785, doi: 10.1016/j.ejrad.2021.109785, indexed in Pubmed: 34091134.
29. D'Agostino D, Casablanca C, Mineo Bianchi F, et al. The role of magnetic resonance imaging-guided biopsy for diagnosis of prostate cancer; comparison between FUSION and "IN-BORE" approaches. Minerva Urol Nephrol. 2021; 73(1): 90–97, doi: 10.23736/S2724-6051.20.03550-X, indexed in Pubmed: 32456413.
30. Wegelin O, van Melick HHE, Hooft L, et al. Comparing Three Different Techniques for Magnetic Resonance Imaging-targeted Prostate Biopsies: A Systematic Review of In-bore versus Magnetic Resonance Imaging-transrectal Ultrasound fusion versus Cognitive Registration. Is There a Preferred Technique? Eur Urol. 2017; 71(4): 517–531, doi: 10.1016/j.eururo.2016.07.041, indexed in Pubmed: 27568655.
31. Prince M, Foster BR, Kaempf A, et al. In-Bore Versus Fusion MRI-Targeted Biopsy of PI-RADS Category 4 and 5 Lesions: A Retrospective Comparative Analysis Using Propensity Score Weighting. AJR Am J Roentgenol. 2021; 217(5): 1123–1130, doi: 10.2214/AJR.20.25207, indexed in Pubmed: 33646819.
32. Maoui M, Gonindard-Melodelima C, Chapet O, et al. Candidates to salvage therapy after external-beam radiotherapy of prostate cancer: Predictors of local recurrence volume and metastasis-free survival. Diagn Interv Imaging. 2021; 102(2): 93–100, doi: 10.1016/j.diii.2020.05.007, indexed in Pubmed: 32534903.
33. Bostwick DG, Meiers I. Diagnosis of prostatic carcinoma after therapy. Arch Pathol Lab Med. 2007; 131(3): 360–371, doi: 10.5858/2007-131-360-DOPCAT, indexed in Pubmed: 17516739.
34. Haj-Hamed M, Karivedu V, Sidana A. Salvage treatment for radio-recurrent prostate cancer: a review of literature with focus on recent advancements in image-guided focal salvage therapies. Int Urol Nephrol. 2019; 51(7): 1101–1106, doi: 10.1007/s11255-019-02114-4, indexed in Pubmed: 30977019.
35. Fuller D, Wurzer J, Shirazi R, et al. Retreatment for Local Recurrence of Prostatic Carcinoma After Prior Therapeutic Irradiation: Efficacy and Toxicity of HDR-Like SBRT. Int J Radiat Oncol Biol Phys. 2020; 106(2): 291–299, doi: 10.1016/j.ijrobp.2019.10.014, indexed in Pubmed: 31629838.
36. Miszczyk L, Stąpór-Fudzińska M, Miszczyk M, et al. Salvage CyberKnife-Based Reirradiation of Patients With Recurrent Prostate Cancer: The Single-Center Experience. Technol Cancer Res Treat. 2018; 17: 1533033818785496, doi: 10.1177/1533033818785496, indexed in Pubmed: 29983098.
37. Wojcieszek P, Szlag M, Głowacki G, et al. Salvage high-dose-rate brachytherapy for locally recurrent prostate cancer after primary radiotherapy failure. Radiother Oncol. 2016; 119(3): 405–410, doi: 10.1016/j.radonc.2016.04.032, indexed in Pubmed: 27165612.